Vol 454|31 July 2008|doi:10.1038/nature07096

LETTERS

Functionalizing hydrogen-bonded surface networks with self-assembled monolayers

Rafael Madueno[1]†, Minna T. Räisänen[1], Christophe Silien[1] & Manfred Buck[1]

One of the central challenges in nanotechnology is the development of flexible and efficient methods for creating ordered structures with nanometre precision over an extended length scale. Supramolecular self-assembly on surfaces offers attractive features in this regard: it is a 'bottom-up' approach and thus allows the simple and rapid creation of surface assemblies[1,2], which are readily tuned through the choice of molecular building blocks used and stabilized by hydrogen bonding[3–8], van der Waals interactions[9], π–π bonding[10,11] or metal coordination[12,13] between the blocks. Assemblies in the form of two-dimensional open networks[3,9,10,13–17] are of particular interest for possible applications because well-defined pores can be used for the precise localization and confinement of guest entities such as molecules or clusters, which can add functionality to the supramolecular network. Another widely used method for producing surface structures involves self-assembled monolayers (SAMs)[18], which have introduced unprecedented flexibility in our ability to tailor interfaces and generate patterned surfaces[19–22]. But SAMs are part of a top-down technology that is limited in terms of the spatial resolution that can be achieved. We therefore rationalized that a particularly powerful fabrication platform might be realized by combining non-covalent self-assembly of porous networks and SAMs, with the former providing nanometre-scale precision and the latter allowing versatile functionalization. Here we show that the two strategies can indeed be combined to create integrated network–SAM hybrid systems that are sufficiently robust for further processing. We show that the supramolecular network and the SAM can both be deposited from solution, which should enable the widespread and flexible use of this combined fabrication method.

We form our supramolecular network from 1,3,5-triazine-2,4,6-triamine (melamine; Fig. 1a) and perylene-3,4,9,10-tetracarboxylic di-imide (PTCDI; Fig. 1b), which form a synthon involving three hydrogen bonds (Fig. 1c). The three-fold symmetry of melamine and the two-fold symmetry of PTCDI give rise to a hexagonal network as shown schematically in Fig. 1d. This bimolecular network is particularly flexible because pore size and shape can be varied by using analogues of PTCDI, and functionality can be added by attaching side groups to the aromatic rings.

So far, the synthesis and further modification of the PTCDI–melamine network have always been performed in an ultra-high-vacuum environment[3,23], which restricts the assembly to molecules that can be sublimed and makes further processing of the network difficult. A solution-based fabrication strategy avoids these limitations and might even allow subsequent processing using SAMs of thiols and related compounds, which offer a plethora of possibilities for surface modification[18,22].

We successfully accomplished a solution-based assembly of the network through adsorption on gold, by using a mixture of PTCDI and melamine in dimethylformamide. The scanning tunnelling microscope (STM) image of the resultant network in Fig. 1e reveals the honeycomb arrangement of the PTCDI molecules, which are the moieties resolved on this scale. The period of the honeycomb is 35 Å, which corresponds to a $(7\sqrt{3} \times 7\sqrt{3})R30^\circ$ unit cell[23]. In contrast to the 50% coverage observed in an earlier ultra-high-vacuum experiment[3], we find that the network forms over extended areas. The network structure overall is very regular and there are no major discontinuities, but some imperfections are discernible. The first, highlighted by the dashed line A in Fig. 1e, is a fault line with neighbouring hexagons meeting at a vertex instead of sharing an edge. The second is an additional PTCDI molecule trapped in a pore (marked by ellipse B). A third imperfection is a missing PTCDI molecule (ellipse C in Fig. 1e), thus joining two adjacent cells.

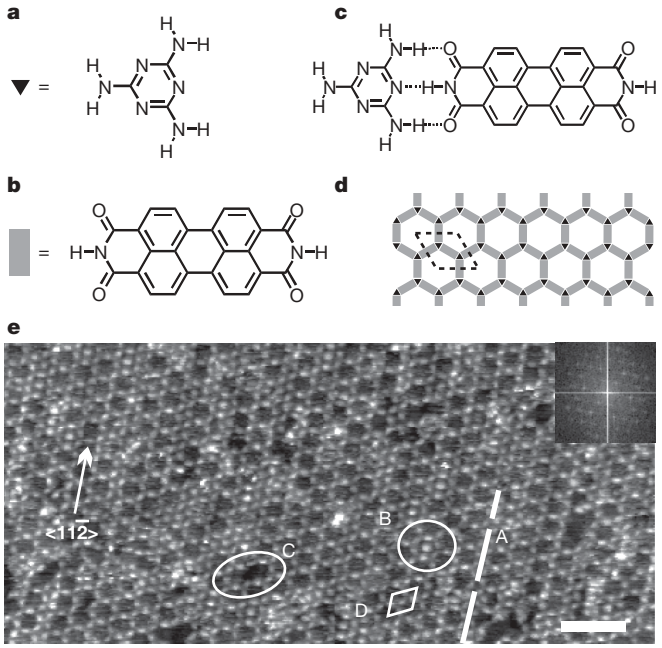

Figure 1 | Supramolecular network of melamine-PTCDI self-assembled on Au(111). a–c, Structures of melamine (**a**) and PTCDI (**b**) and the bonding motif (**c**). **d**, Schematic diagram of the network with the unit cell indicated by a dotted rhombus. **e**, STM image of network recorded in ambient conditions. The dashed line A highlights a fault line. Circled areas B and C mark a pore hosting a PTCDI molecule and a missing PTCDI molecule, respectively. The $(7\sqrt{3} \times 7\sqrt{3})R30^\circ$ unit cell (D) corresponding to a 35-Å period of the honeycomb is also indicated. The inset shows a Fourier transform. Scale bar, 10 nm.

[1]EaStCHEM School of Chemistry, University of St Andrews, North Haugh, St Andrews KY16 9ST, UK. †Present address: Departamento de Química Física, Universidad de Córdoba, Campus de Rabanales, 14014 Cordoba, Spain.

The solution-based preparation makes the network a readily available template, but the scope for further modification and use depend on its stability under the conditions of subsequent processing. As illustrated in Fig. 2a, we aim for further modification with SAMs. A precise estimation of network stability under relevant conditions is not possible because of the lack of precise data for the network, in particular for the adsorption energies of PTCDI and melamine. However, we can use the hydrogen-bond energy per synthon (values range from 70 kJ mol^{-1} (ref. 24) to 90 kJ mol^{-1} (ref. 25)) to calculate total network binding energies of 140–180 kJ mol^{-1} and 210–270 kJ mol^{-1} per PTCDI and melamine molecule, respectively. The adsorption energies of PTCDI and melamine are taken to be similar to those of other aromatic hydrocarbons[26,27], which range from 50 to 200 kJ mol^{-1}. With this approach, we estimate the binding energy of a network molecule to fall in the range 200–470 kJ mol^{-1}, which is higher than the 160–200 kJ mol^{-1} of an Au–S bond[18,22]. However, considering that more than one thiol molecule can be adsorbed in the area occupied by PTCDI and melamine, we conclude that thiol adsorption can match the network energetically.

To investigate to what extent thiols can be adsorbed in the network we chose three types of molecule (see Fig. 2b) differing in the stability of the respective SAMs. One is small and rigid and has rather weak intermolecular interactions (adamantane thiol; ASH)[28]; the other two show more pronounced intermolecular interactions, one consisting of a rigid aromatic moiety combined with an aliphatic spacer (ω-(4′-methylbiphenyl-4-yl)propane thiol; BP3SH) and the other of a flexible alkane chain (dodecane thiol; C12SH). Large-scale STM images of the resultant structures (Fig. 2c–e) show that the network acts as template for all three types of molecule, with high-resolution images and Fourier transforms (see insets) confirming that in all cases the hexagonal pattern is well maintained after thiol adsorption. In contrast to the empty network, in which the molecules appear as protrusions (Fig. 1), filling the network pores inverts the height contrast so that the presence of the network is reflected by the appearance of hexagonal grooves. It is worth noting that as a result of the rigidity of adamantane thiol it was even possible to achieve molecular resolution (Fig. 2c, inset).

Figure 2 demonstrates that the supramolecular network serves as a general template for a range of thiol molecules that form SAMs differing substantially in structure, intermolecular interactions and stability. However, we note that the details of the preparation protocol are dependent on the SAM molecule used, and reflect the above estimated similarity of SAMs and network with regard to their energetics. For adamantane thiol, which is known to form SAMs that are not very stable (in comparison with SAMs formed from alkane thiols, for example), immersion time is not critical: the pores of the network are filled within seconds, and the network itself is perfectly stable against displacement by ASH. In contrast, for the other two molecules, prolonged exposure of the network to a solution of the respective thiol molecules ultimately results in the displacement of the network and the formation of a uniform SAM. However, there is a pronounced difference between the rate at which the pores are filled and the rate at which the network is displaced, so that selective adsorption in the pores while maintaining the network structure can be controlled kinetically, as demonstrated by Fig. 2.

Once formed, the SAM–network hybrid structure is stable in a liquid environment and can be processed further, as we illustrate here with the electrochemical deposition of Cu in the underpotential deposition (UPD) region. The experiment, sketched in Fig. 3a, involves the mounting of a sample with the SAM–network hybrid in an electrochemical cell containing Cu^{2+} ions. A potential in the UPD region of Cu (that is, positive of the Nernst potential) is then

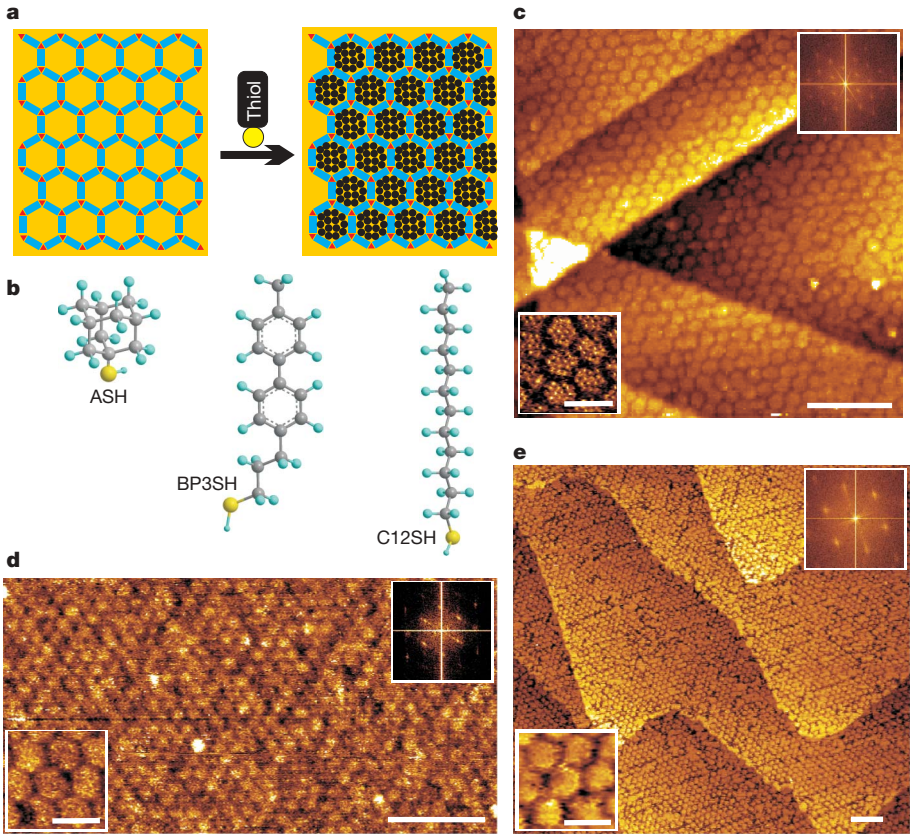

Figure 2 | Generation of a network–SAM hybrid structure. **a**, Scheme of filling the cells of the PTCDI–melamine network by thiols. **b**, Structures of the thiols studied. **c**–**e**, STM images of the hybrid structures on Au(111)/mica: network filled with ASH (**c**), C12SH (**d**) and BP3SH (**e**). The insets at the lower left and upper right corners of the STM images show high-resolution images and Fourier transforms, respectively. Scale bars, 20 nm (large-scale images) and 5 nm (insets).

applied, which causes the insertion of a monolayer of Cu between the Au substrate and the thiol molecules[29]. The Cu insertion renders the thiol–substrate bond more stable and could be used for further patterning[30]. After deposition, the sample was removed from the cell and investigated by STM in ambient environment, with the image (Fig. 3b) revealing that the pattern of the hybrid structure is preserved.

To probe the insertion of Cu, experiments were performed with a deposition time chosen such that Cu UPD had not yet occurred homogeneously across the whole sample. In the STM image (Fig. 3c), the hexagonal structure is discernible in both the unaltered and the UPD areas. In contrast, the corresponding height profile (Fig. 3d) reveals an increase in height S as a result of Cu UPD. A particular feature of Fig. 3d is the difference in the corrugation between the UPD and the unaltered area, respectively. On the UPD part the corrugation A is significantly larger than the corrugation B of the unaltered area. This strongly suggests that Cu is inserted only between thiol and substrate and not between network and substrate as illustrated in Fig. 3a; that is, the network acts as a diffusion barrier. This interpretation is corroborated by the appearance of isolated UPD islands (marked by arrows in Fig. 3c) in which only one cell is filled. The suppression of Cu diffusion at the interface by the network makes the hybrid system very different from a uniform SAM in which Cu UPD cannot be confined because of the lack of such a diffusion barrier[29]. We also note that, in comparison with densely packed SAMs, intercalation of the Cu ions at the thiol/substrate interface is greatly facilitated and faster for the hybrid system as a result of the more open structure. Overall, the hybrid system renders UPD on the nanometre scale much more controllable than when using a SAM without network.

The results presented here show that the honeycomb network involving three hydrogen bonds per synthon demonstrates sufficient stability to act as template in subsequent processes. The combination of the network with SAMs offers considerable design flexibility, with the network providing an exact definition of structures in the substrate plane and the SAM permitting separate surface modification. Whether the SAM-modified pores serve as active sites for a precise localization of species through chemical interactions or whether they are used as blocking sites to direct species to the network molecules, the hybrid system can provide control on a length scale and at a precision not readily achievable otherwise. We believe that this feature, and the fact that the hybrid system is accessible through exclusively solution-based processing, will facilitate a wide range of fundamental studies into how confined nanometre-sized geometries can influence phenomena as diverse as electrochemistry, tribology and wetting.

METHODS SUMMARY

PTCDI (at least 98% pure; Alfa Aesar) and melamine (99.9% pure; Sigma-Aldrich) were used without further purification. The mixture of PTCDI and melamine used for the experiments was prepared from saturated solutions of PTCDI and melamine in dimethylformamide that were diluted, typically 1:25 and 1:4, respectively. Au/mica substrates (300 nm gold; Georg Albert PVD) were flame-annealed before immersion in the PTCDI/melamine solution. Immersion times for network formation were up to 3 min at temperatures between 325 and 400 K, with 1 min and 371 K as a typical combination of parameters. After removal from solution, samples were blown dry in a stream of nitrogen or argon. For thiol adsorption experiments, network/Au/mica samples were immersed in a 1 mM solution of the respective thiol (ASH (99.9% pure; Sigma-Aldrich), C12SH (at least 98% pure; Sigma-Aldrich) or BP3SH (for synthesis see ref. 43 in ref. 29)) in ethanol at 18–21 °C. Immersion times were varied between 3 s and 24 h. After immersion, samples were thoroughly rinsed with ethanol and blown dry with nitrogen.

Partial Cu UPD was achieved in 50 mM $CuSO_4$, 0.5 μM H_2SO_4 (aqueous) by setting the sample potential at +100 mV against Cu/Cu^{2+} for 10 s in a polytetrafluoroethylene electrochemical cell. The sample was then rinsed with

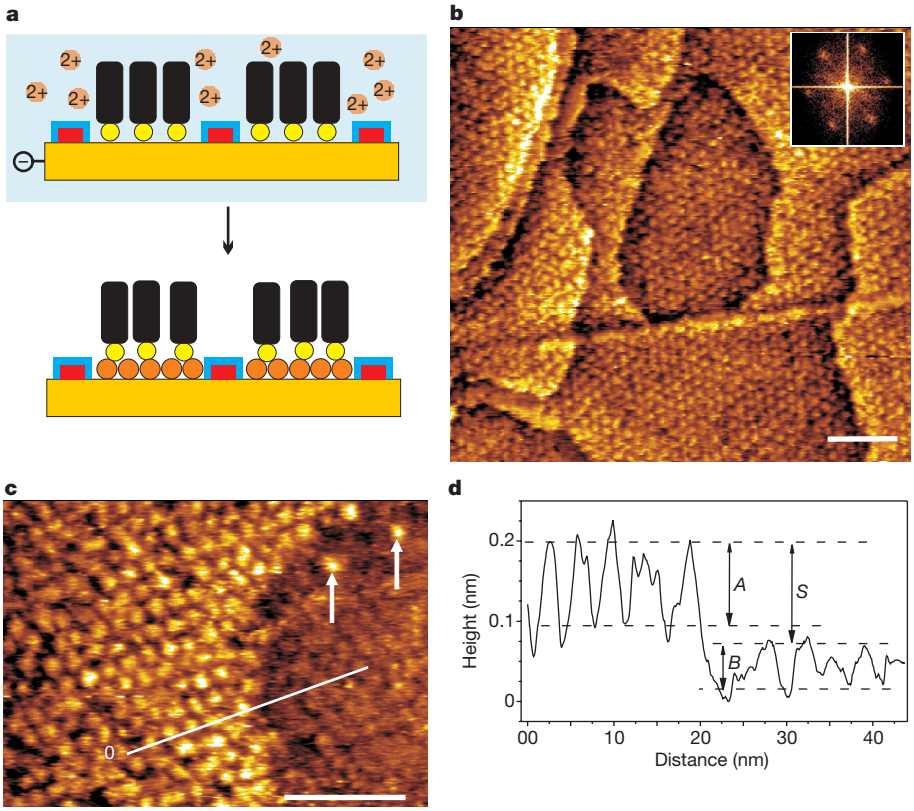

Figure 3 | UPD of Cu on Au(111) modified by an adamantane-thiol-filled PTCDI–melamine network. **a**, Illustration of electrochemical Cu deposition in pores of the network at the thiol/Au interface. **b**, **c**, STM images of samples taken in ambient atmosphere after Cu UPD: complete UPD (**b**) and partial UPD (**c**). Scale bars, 20 nm. Arrows in **c** mark isolated cells of Cu UPD. **d**, Height profile along the line given in **c**, with the origin marked by '0'. Corrugations are $A = 1.15$ Å on UPD areas and $B = 0.5$ Å on unaltered areas. The height difference between UPD and unaltered areas is $S = 1.3$ Å.

deionized water and blown dry with nitrogen. Complete Cu UPD coverage was achieved by repeating the same procedure once.

Samples were characterized under ambient by STM with a PicoPlus STM (Molecular Imaging). Bias and currents were typically in the range 250–800 mV (tip positive) and 5–80 pA. Figure 1e is despeckled, all other images are presented as acquired.

Received 3 December 2007; accepted 9 May 2008.

1. De Feyter, S. & De Schryver, F. C. Two-dimensional supramolecular self-assembly probed by scanning tunneling microscopy. *Chem. Soc. Rev.* **32,** 139–150 (2003).
2. Barth, J. V. Molecular architectonic on metal surfaces. *Annu. Rev. Phys. Chem.* **58,** 375–407 (2007).
3. Theobald, J. A., Oxtoby, N. S., Phillips, M. A., Champness, N. R. & Beton, P. H. Controlling molecular deposition and layer structure with supramolecular surface assemblies. *Nature* **424,** 1029–1031 (2003).
4. Li, Z., Han, B., Wan, L. J. & Wandlowski, T. Supramolecular nanostructures of 1,3,5-benzene-tricarboxylic acid at electrified Au(111)/0.05 M H_2SO_4 interfaces: An *in situ* scanning tunneling microscopy study. *Langmuir* **21,** 6915–6928 (2005).
5. Pinheiro, L. S. & Temperini, M. L. A. Pyridine and pyridine carboxylic acids as guests in a bidimensional hydrogen bond structure analyzed by scanning tunneling microscopy. *Surf. Sci.* **601,** 1836–1843 (2007).
6. Canas-Ventura, M. E. *et al.* Self-assembly of periodic bicomponent wires and ribbons. *Angew. Chem. Int. Ed.* **46,** 1814–1818 (2007).
7. Payer, D. *et al.* Ionic hydrogen bonds controlling two-dimensional supramolecular systems at a metal surface. *Chem. Eur. J.* **13,** 3900–3906 (2007).
8. Kampschulte, L., Griessl, S., Heckl, W. M. & Lackinger, M. Mediated coadsorption at the liquid–solid interface: Stabilization through hydrogen bonds. *J. Phys. Chem. B* **109,** 14074–14078 (2005).
9. Furukawa, S. *et al.* Structural transformation of a two-dimensional molecular network in response to selective guest inclusion. *Angew. Chem. Int. Ed.* **46,** 2831–2834 (2007).
10. Mena-Osteritz, E. & Bäuerle, P. Complexation of C_{60} on a cyclothiophene monolayer template. *Adv. Mater.* **18,** 447–451 (2006).
11. Schenning, A. & Meijer, E. W. Supramolecular electronics; nanowires from self-assembled π-conjugated systems. *Chem. Commun.* 3245–3258 (2005).
12. Diaz, D. J., Bernhard, S., Storrier, G. D. & Abruna, H. D. Redox active ordered arrays via metal initiated self-assembly of terpyridine based ligands. *J. Phys. Chem. B* **105,** 8746–8754 (2001).
13. Stepanow, S. *et al.* Steering molecular organization and host–guest interactions using two-dimensional nanoporous coordination systems. *Nature Mater.* **3,** 229–233 (2004).
14. Stöhr, M., Wahl, M., Spillmann, H., Gade, L. H. & Jung, T. A. Lateral manipulation for the positioning of molecular guests within the confinements of a highly stable self-assembled organic surface network. *Small* **3,** 1336–1340 (2007).
15. Spillmann, H. *et al.* A two-dimensional porphyrin-based porous network featuring communicating cavities for the templated complexation of fullerenes. *Adv. Mater.* **18,** 275–279 (2006).
16. Lu, J. *et al.* Template-induced inclusion structures with copper(II) phthalocyanine and coronene as guests in two-dimensional hydrogen-bonded host networks. *J. Phys. Chem. B* **108,** 5161–5165 (2004).
17. Stepanow, S. *et al.* Surface-assisted assembly of 2D metal-organic networks that exhibit unusual threefold coordination symmetry. *Angew. Chem. Int. Ed.* **46,** 710–713 (2007).
18. Schreiber, F. Self-assembled monolayers: from 'simple' model systems to biofunctionalized interfaces. *J. Phys. Condens. Matter* **16,** R881–R900 (2004).
19. Gooding, J. J., Mearns, F., Yang, W. R. & Liu, J. Q. Self-assembled monolayers into the 21st century: Recent advances and applications. *Electroanal.* **15,** 81–96 (2003).
20. Mrksich, M. A surface chemistry approach to studying cell adhesion. *Chem. Soc. Rev.* **29,** 267–273 (2000).
21. Thom, I., Hähner, G. & Buck, M. Replicative generation of metal microstructures by template directed electrometallization. *Appl. Phys. Lett.* **87,** 024101 (2005).
22. Love, J. C., Estroff, L. A., Kriebel, J. K., Nuzzo, R. G. & Whitesides, G. M. Self-assembled monolayers of thiolates on metals as a form of nanotechnology. *Chem. Rev.* **105,** 1103–1170 (2005).
23. Perdigao, L. M. A. *et al.* Bimolecular networks and supramolecular traps on Au(111). *J. Phys. Chem. B* **110,** 12539–12542 (2006).
24. Weber, U. K. *et al.* Role of interaction anisotropy in the formation and stability of molecular templates. *Phys. Rev. Lett.* **100,** 156101 (2008).
25. Aakeroy, C. B. & Seddon, K. R. The hydrogen-bond and crystal engineering. *Chem. Soc. Rev.* **22,** 397–407 (1993).
26. Baldacchini, C., Mariani, C. & Betti, M. G. Adsorption of pentacene on filled d-band metal surfaces: Long-range ordering and adsorption energy. *J. Chem. Phys.* **124,** 154702 (2006).
27. Bilic, A., Reimers, J. R., Hush, N. S., Hoft, R. C. & Ford, M. J. Adsorption of benzene on copper, silver, and gold surfaces. *J. Chem. Theory Comput.* **2,** 1093–1105 (2006).
28. Dameron, A. A., Charles, L. F. & Weiss, P. S. Structures and displacement of 1-adamantanethiol self-assembled monolayers on Au{111}. *J. Am. Chem. Soc.* **127,** 8697–8704 (2005).
29. Silien, C. & Buck, M. On the role of extrinsic and intrinsic defects in the underpotential deposition of Cu on thiol-modified Au(111) electrodes. *J. Phys. Chem. C* **112,** 3881–3890 (2008).
30. Oyamatsu, D., Kanemoto, H., Kuwabata, S. & Yoneyama, H. Nanopore preparation in self-assembled monolayers of alkanethiols with use of the selective desorption technique assisted by underpotential deposition of silver and copper. *J. Electroanal. Chem.* **497,** 97–105 (2001).

Acknowledgements We are grateful to J. D. E. T. Wilton-Ely for his contribution to the synthesis of BP3SH. This work was supported by the UK Engineering Physical Sciences Research Council (EPSRC). M.R. acknowledges support from the Academy of Finland.

Author Contributions All authors contributed to the design of the experiments. The preparation and characterization of networks and hybrid systems were performed by R.M and M.T.R.. Experiments and analysis related to electrochemistry were conducted by C.S. All authors contributed to the manuscript, with M.B. and R.M. leading.

Author Information Reprints and permissions information is available at www.nature.com/reprints. Correspondence and requests for materials should be addressed to M.B. (mb45@st-and.ac.uk) or R.M. (rafael.madueno@uco.es).